

COMPARISON OF ACOUSTIC AND STRAIN GAUGE
TECHNIQUES
FOR CRACK CLOSURE MEASUREMENTS

By Otto Buck, R. V. Inman, and J. D. Frandsen

Prepared under Contract No. NAS1-13883
ROCKWELL INTERNATIONAL
Science Center
P. O. Box 1085
Thousand Oaks, California 91360

for

NATIONAL AERONAUTICS AND SPACE ADMINISTRATION

SC5032.22FR

COMPARISON OF ACOUSTIC AND STRAIN GAUGE
TECHNIQUES
FOR CRACK CLOSURE MEASUREMENTS

Final Report

Covering Period
April 17, 1975 through December 31, 1975

Prepared under Contract No. NAS1-13883
General Order 5032

Prepared for

NATIONAL AERONAUTICS AND SPACE ADMINISTRATION
Langley Research Center
Hampton, Virginia

by

Otto Buck, R. V. Inman, and J. D. Frandsen



Science Center
Rockwell International

1049 CAMINO DOS RIOS
THOUSAND OAKS, CALIF. 91360
805/498-4545

TABLE OF CONTENTS

	<u>Page</u>
Foreword	ii
I. INTRODUCTION	1
II. TECHNICAL	2
A. Task 1.1 - Part-Through Crack Specimen	2
B. Task 1.2 - Compact Tension Specimen	5
III. COMPRESSION TESTS	8
A. Task 2.1 - Contact Area/Sphere	8
B. Task 2.2 - Contact Area/Cylinders	10
IV. CONCLUSIONS	12
V. REFERENCES	13

FIGURES

Figures 1 through 21

FOREWORD

A quantitative study on the systems performances of the NASA COD gauge and the acoustic transmission techniques to elastic deformation of part-through crack and compact-tension specimens has been conducted. It is shown that the two instruments measure two completely different quantities: The COD gauge yields information on the length change of the specimen whereas the acoustic technique is sensitive directly to the amount of contact area between two surfaces, interfering with the acoustic signal. In another series of experiments, compression tests on parts with specifically prepared surfaces were performed so that the surface contact area could be correlated with the transmitted acoustic signal, as well as the acoustic with the COD gauge signal. A linear relation between contact area and COD gauge signal was obtained until full contact had been established.

SC5032.22FR

I. INTRODUCTION

Crack closure at positive stress levels (1) presently is being considered as a possible mechanism to explain changes in fatigue crack propagation rates caused by variations in the testing conditions. In general, all sensors (1-11) used to monitor fatigue crack growth also yield some information about crack closure. A typical example (11) of closure as it occurs on a compact tension specimen is given in Fig. 1 using the NASA COD gauge (bottom) and the transmitted, as well as the reflected acoustic wave signal. In all cases, crack closure is initiated at some load level (the closure load P_0) and increases rapidly as the load decreases. The previously used method of defining P_0 for the acoustic signals (10) has been to use the intersection of tangents to the two extreme segments of the curves. In the present example (Fig. 1) this agrees well with the point where nonlinearity is first observed using the NASA COD gauge. One might argue then that there is good agreement between the two techniques. This conclusion is unsatisfactory, however, since two different definitions for P_0 have been used.

The present report describes the results of a study designed to compare two sensing techniques, the NASA COD gauge technique (1) and the acoustic wave transmission technique (9), (11). The experiments have been performed on both part-through crack (PTC) (see Task 1.1) and compact tension (CT) specimens (see Task 1.2) into which artificial notches or slits, simulating true fatigue cracks, had been introduced by electrical discharge machining (EDM) or sawing, respectively. Tension-tension loading was applied to the specimens during these tests. Since the artificial notches are relatively wide (0.2-0.5 mm) no crack closure can be observed during these tests, however. To simulate crack closure a special compression jig was constructed. Using this jig, two kinds of experiments were performed: In the first experiment (Task 2.1) a half-sphere made out of a high-strength aluminum alloy was pressed into a well-annealed aluminum plate and the contact area as well as the transmitted acoustic signal determined. In the second experiment (Task 2.2) two well-annealed flat aluminum plates were pressed against each other and the transmitted acoustic signal as well as the COD gauge output determined.

SC5032.22FR

In the following, the conditions and the results of the experiments performed will be described. Each task is treated individually according to the work statement of this contract, with the first two tasks devoted to the technical evaluation of the equipment on the notched samples and with the second two tasks dealing with observations obtained on simple compression tests.

II. TECHNICAL EVALUATION OF EQUIPMENT

A. Task 1.1 - Part-Through Crack Specimen

The objective of this task was to compare the response of the acoustic surface wave device (ASWD - 0.5 MHz), extensively described in Ref. 9, and that of the NASA COD gauge, extensively described in Ref. 1, applied to a part-through crack (PTC) specimen. The geometry of the PTC specimen (A1 2219-T851) was 1.25 cm thick, 10 cm wide, and a gauge length of 20 cm. A semi-elliptical notch, about 0.25 mm deep, with an aspect ratio, $a/2c$, of about 1:3 was cut into the specimen by EDM (the notch depth was increased after each test and depth will be quoted with the results). Both ASWD and COD were first placed onto the unnotched side of the specimen, across from the notch. The specimen was then loaded in an MTS electro-hydraulic system with the loading axis perpendicular to the notch (Mode I) using a triangular load-time relation. One full load cycle required 100 sec. This procedure was chosen since it was decided to form the load derivative of the signal outputs. Electronically, it is easy to obtain the time derivative; thus the above method is useful to achieve the stated goal. Both ASWD and COD were then placed over the EDM notch and the same test procedures used as outlined above.

Since it took only a few load cycles to obtain the necessary data, fatigue cracks were not initiated in any case. Consequently, crack closure should not and was not observed. Observations of crack closure under similar conditions have been reported earlier however. (11) Typical examples of COD gauge and ASWD signal output (in volts) as well as their respective differentiated signals (also in volts) are shown in Figs. 2 and 3 as a function of applied load. The major difference in their response

SC5032.22FR

to load is quite obvious: The COD gauge is sensitive to the compliance of the specimen, whereas the ASWD is not. This is not a surprising result since the two instruments measure two completely different quantities. The COD gauge yields information on the length change of the specimen and the ASWD information on the acoustic attenuation change - e.g., due to an increase of crack length or due to closure of a crack, both of which change the local cross-sectional area through which the acoustic energy has to pass. This leads, basically, to a strong advantage of the ASWD over the COD gauge. Information on crack closure to be deduced from the COD gauge has to be subtracted out from the purely elastic component of response (Fig. 2), whereas the ASWD yields this information directly since there is no elastic response component (Fig. 3). Therefore, one may view the ASWD output signal as similar to the differentiated COD gauge signal. Thus it was decided to build an electronic differentiator and compare the load differential of the COD gauge signal (Fig. 2) directly with the ASWD signal (Elber (12) has given an alternative method to observe deviations from the linear behavior by calculating reduced displacements which are a deviation from the line of best fit to the loading curve). Unfortunately, the noise level of the COD gauge is relatively large, which is amplified in the differentiated signal. Further work would be necessary to eliminate these problems (electrical shielding of the COD gauge might be a solution).

In a series of experiments the COD gauge and ASWD outputs as a function of the depth of EDM notches was determined (see Figs. 4 and 5, respectively). The COD gauge output in Fig. 4 is directly given in μm , by calibrating the COD gauge on a micrometer screw equipped test jig. Additional data not shown in Fig. 4 have been produced with the gauge mounted way off the plane of the notch. The modulus of elasticity determined in the latter test was found to be only 0.8% less than the one given in standard materials handbooks. The ASWD signal in this case (no notch intercepting the acoustic path) was found to be $(4.4 \pm 0.1)\text{V}$. The COD gauge data taken opposite the notch (denoted by $a = 0\text{ mm}$) already reflect the increased compliance due to the notch: The compliance is increased by about 25% over the value yielding the true modulus of elasticity of the material. The ASWD signal does not show such an effect. The signal level is still about 4.4V. (If the notch would be deeper than 7 mm, it could be recognized by the ASWD, however.)

SC5032.22FR

The stiffness (defined as the inverse of the compliance), as measured by the COD gauge, and the ASWD signal decrease as the depth of the notch is increased. This is shown in Fig. 6, with both quantities normalized at $a = 0$ mm. The figure indicates that for the COD gauge the percentage change in stiffness at a small notch depth ($a < 2$ mm) is larger than the percentage change in the ASWD signal. At larger notch depths ($a > 2$ mm) the situation is reversed. This behavior is not unexpected since the COD gauge signal change is proportional to the change in crack length (or crack area) whereas the ASWD signal change is proportional to the change in net area.

An experimental advantage of the COD gauge over the ASWD becomes apparent in this figure: The ASWD data show a large scatter if the device is removed and remounted to the specimen. (In actual crack propagation measurements the device is calibrated without removing it from the specimen using the standard fracture mechanics marker method.)

Systems performances for both COD gauge and ASWD as applied to a PTC specimen are as follows:

(a) Mechanical Range

COD gauge: 0.15 mm in compression
 0.10 mm in tension

(determined from the first deviation from linearity in the calibration test jig).

ASWD: Unlimited, unless Poisson's contraction reduces the cross-section to the depth of the surface wave penetration.

(b) Sensitivity (derived from Fig. 6)

For both devices sensitivity is a function of device and electronics. The following numbers are quoted in percentage change in output per mm crack extension.

Crack Depth	0 mm	1 mm	2 mm	3 mm	4 mm
COD Gauge	500%/mm	43%/mm	40%/mm	24%/mm	20%/mm
ASWD	4%/mm	8%/mm	21%/mm	92%/mm	325%/mm

SC5032.22FR

(c) Resolution

COD Gauge: corresponding to $5 \times 10^{-1} \mu\text{m}$ of crack extension.

ASWD: corresponding to $5 \mu\text{m}$ crack extension (if calibrated using the marker technique (10)).

(d) Stability

COD gauge: Taking nine readings over 24 hrs the stability was determined to be equivalent to $\pm 4 \mu\text{m}$ crack extension per 24 hrs.

ASWD: Taking nine readings over 24 hrs the stability was determined to be equivalent to $\pm 50 \mu\text{m}$ crack depth.

(e) Linearity

COD gauge: Maximum deviation from a straight line of the COD gauge output as a function of load (Fig. 4) over the tested range of notch depths did not exceed 0.5%.

ASWD: Maximum change of the ASWD output as a function of load (Fig. 5) over the tested range of notch depths did not exceed 0.5%.

(f) Noise

COD gauge: corresponding to $3.5 \mu\text{m}$ crack extension.

ASWD: corresponding to $5 \mu\text{m}$ crack extension (if calibrated using the marker technique (10)).

The above comparison seems to favor the COD gauge over the ASWD. It has to be kept in mind, however, that the COD gauge signal usually has to be processed (differentiated) to obtain crack closure data. Processing may change the above quantities such that the apparent advantage of the COD becomes less. It has also to be kept in mind that the two devices measure different physical quantities, as mentioned earlier, which seem to favor the ASWD measurements (11).

B. Task 1.2 - Compact Tension Specimen

The objective of this task was to compare the response of the acoustic transmission technique (ATT = 2.0 MHz, extensively described in Ref. 11) and that of the NASA COD gauge (1) applied to a compact tension (CT)

SC5032.22FR

specimen. The geometry of the CT specimen (A1 2219-T851) was (13) $W = 11.3$ cm, $2h = 11.0$ cm, and $B = 2.54$ cm. Using a bandsaw a slit about 0.5 mm wide was cut into the specimen (along the plane on which the fracture would occur during fatigue). (The slit depth was increased after each test and numbers will be quoted with the results.) The ATT was placed such (11) that the slits blocked out 50% of the transmitted acoustic wave (which means the transmitter and receiver had to be moved as the slit depth changed). The COD gauge was always placed 2.5 mm behind (across the saw cut) the tip of the slit (11). The specimen was then loaded in the MTS system perpendicular to the notch, again using a triangular load-time relation, with a full load cycle requiring 100 sec.

Fatigue cracks were not initiated in any case. Therefore, crack closure should not and was not observable. Such observations have been reported earlier, however (11). Similar to the statements made in Task 1.1, the COD gauge is sensitive to the stiffness of the specimen (at the location of the gauge), whereas the ATT is not.

In a series of experiments the response of both COD gauge and ATT outputs as a function of the length of a saw cut was determined (see Figs. 7 and 8, respectively). The COD gauge output in Fig. 7 is directly given in μm (note the changing load scale in this figure). The average slope of these curves, in general, increases with increasing saw cut depth. It is also very sensitive to the location of the COD gauge with respect to the tip of the cut, which leads to some inconsistency: The inverse behavior of the slope for $a = 40$ and $a = 45$ mm is due to an inaccuracy in gauge positioning. One of the main features, different from the data obtained on the PTC specimen (Fig. 4), is the relatively large nonlinearity observed at low load levels. To check if this effect is specific to the COD gauge arrangement on the CT specimen a regular commercial clip-on gauge was mounted to the mouth of the specimen and a similar nonlinear behavior was observed. The reason for this nonlinearity is unknown at the present time.

SC5032.22FR

The ATT output signals obtained during the experiments are shown in Fig. 8. In general, the signals as a function of load decrease slightly which is caused by a slight bending of the specimen reducing the coupling of the transducers to the specimen.

Systems performance for both COD gauge and ATT as applied to a CT specimen are as follows:

(a) Mechanical Range

COD gauge: 0.15 mm in compression

0.10 mm in tension

(determined from the first deviation from linearity in the calibration test jig)

ATT: Limited by the curvature of the bonding surface of the CT specimen at maximum applied load. Flexible transducers would overcome these difficulties.

(b) Sensitivity

For both devices sensitivity is a function of device and electronics. The following numbers are quoted in percentage change in output per mm crack extension (averaged between $a = 20$ mm and 45 mm - see Fig. 7).

COD gauge: 2.2%/mm

ATT: 10%/mm

(c) Resolution

COD gauge: corresponding to $1\mu\text{m}$ of crack extension.

ATT: $5\mu\text{m}$ crack extension (if calibrated using the marker technique (10)).

(d) Stability

COD gauge: Taking nine readings over 24 hrs the stability was determined to be equivalent to $\pm 4\mu\text{m}$ crack extension per 24 hrs.

ATT: Taking nine readings over 24 hrs the stability was determined to be equivalent to $\pm 50\mu\text{m}$ crack depth.

SC5032.22FR

(e) Linearity

COD gauge: Deviation from a straight line of the COD gauge output as a function of load (Fig. 7) over the tested range of saw cut depths was determined to be about 20%.

ATT: Maximum change of the ATT output as a function of load (Fig. 8) over the tested range of saw cut depths was determined to be about 1.5%.

(f) Noise

COD gauge: corresponding to $3.5\mu\text{m}$ crack extension.

ATT: corresponding to $5\mu\text{m}$ crack extension (if calibrated using the marker technique (10)).

Remarks about this comparison similar to the ones in Section 1.1 are applicable.

III. COMPRESSION TESTS

A. Task 2.1 - Contact Area/Sphere

The objective of this task was to press a spherical cap made out of a high strength aluminum alloy (7075-T6) into a soft flat plate of aluminum (well annealed Al 1100) and to determine the transmission of an acoustic wave (ATT - 1 MHz) as a function of contact area.

The compression jig used in these experiments is shown in Figs. 9 and 10: 1 MHz longitudinal PZT transducers were mounted in cavities of cylindrical Al 7075-T6 "transducer holders" (A and B in Fig. 9, with the cavity visible at B). C and D are the well annealed Al 1100 flat plate and the high strength Al 7075-T6 spherical cap, respectively. Both pieces were each waxed to one of the transducer holders (A shows one of the smaller cylindrical specimens used in Task 2.2 waxed to a transducer holder). Both combined parts were then inserted into a "teflon guide piece" E such that the spherical cap was facing the well annealed 1100 flat plate. The COD gauge F was not used in this experiment. The assembled test jig (including the mounted COD gauge) is shown in Fig. 10. As can be seen there, the teflon guide piece was somewhat shorter in length than the two combined parts together so that, if inserted into the MTS hydraulic system, the compressional load would just act upon the metallic parts and not on the teflon guide piece.

SC5032.22FR

A typical example of the ATT output signal as a function of load is shown in Fig. 11. The signal increases very rapidly at low load levels and saturates at the high levels. Some hysteresis in the signal is observed as the load cycle is completed. The load independent part of the signal output is interpreted as a consequence of full contact established between the spherical cap and the impression it made into the soft flat plate. A light microscope picture of such an impression is shown as insert in Fig. 11. The ATT output signal indicates that during the unloading the sphere stays in full contact between 5.6 and 3×10^3 N. Below 3×10^3 N the contact area diminishes, probably due to a strain relaxation in the flat plate. There are no means to correlate actual contact area and signal level in any such experiment except at the saturation level. Thus a series of experiments similar to the one shown in Fig. 11 had to be made, starting out with a low maximum load level. After each experiment the projected impression of the spherical cap was determined and correlated with the saturation level. The result is shown in Fig. 12. Up to about a signal level of 3.5V it is approximately linear with the contact area. Thereafter it deviates from this initial behavior, mainly due to a nonlinear response of the peak detector circuit. In the same figure, average stress data obtained at maximum load and calculated from the maximum applied load and the projected contact area as a function of contact area have been plotted. Probably due to the work hardening characteristic of the flat plate material some increase in the stress level is observed as the contact area (or the maximum load level) is increased. Having established the ATT signal versus contact area relationships at maximum load level (as shown in Fig. 12) it seems feasible to replot the ATT output signal versus load (an example of which is shown in Fig. 11) in the form contact area versus load or, even further, in the form contact area versus applied stress. The latter result is shown in Fig. 13 for the unloading part of all experiments carried out. After an almost linear relationship at the low levels, each curve saturates which, as has been mentioned before, is interpreted as full contact between spherical cap and its indentation being established.

SC5032.22FR

B. Task 2.2 - Contact Area/Cylinders

The objective of this task was to press two cylinders, made out of well annealed Al 1100, against each other and to determine the transmission of an acoustic wave (ATT - 1 MHz) with the output of the COD gauge, put across the interface of the two cylinders (1.25 cm diameter), as a function of applied load. As may be seen in the following these experiments have been designed to simulate crack closure. The compression jig used in these experiments has been discussed already in the previous task (Figs. 9 and 10). At A in Fig. 9 one of these cylinders is shown, waxed to a transducer holder. Figure 10 shows the fully assembled compression test jig, including the COD gauge.

Some results of the ATT output signal as well as the COD gauge output (calibrated in displacement) as a function of applied load for an increasing maximum load level are shown in Figs. 14-17 (note the changing load scale). As can be seen the biggest change in the COD gauge output occurs at the very low load levels where the ATT signal does not change yet, indicating a thin air gap which has to be closed in thickness or in area or both before transmission can occur. At zero load contact between the two cylinders exists at a few spots only. In this series of experiments the ATT signal indicates full contact at a load of about 2000N (Fig. 16). Further increase of the maximum load shows a slight decrease in the ATT signal (Fig. 17), the reason for which is unknown at present. A similar decrease of the acoustic signal has been observed in crack closure studies reported earlier (13). Further experiments using the present technique might be useful to determine the cause of this effect. The COD gauge output showed very little hysteresis (Figs. 14-17). As the maximum load reached 4800N ($\sigma \approx 39 \text{ N/mm}^2$, a stress close to the yield stress of this material) the COD gauge started to show some hysteresis and an offset at the maximum load level. Examples of this behavior are shown in Fig. 18. The offset at minimum load level decreases if exactly the same load cycle is repeated which indicates that the effect is due to plastic yielding. Thus plastic yielding cannot be noticed in the ATT signal as shown by the example of the ATT signal in Fig. 18 which has been recorded simultaneously with the third COD gauge loop shown in this figure.

SC5032.22FR

After these initial experiments the maximum load level was decreased again to the level used in Fig. 17. The results are shown in Fig. 19 where the ATT signal now indicates full contact of the surfaces at about half the load level that was required before. The COD gauge showed some offset at the minimum load level, the reason for which is unknown at the present time. The differentiated signals of Fig. 19 are shown in Fig. 20. The large changes of the ATT signal over those observed with the COD gauge again are reflected in the differentiated signals. The load level at which maximum contact of the cylindrical surfaces is achieved may be defined by a zero slope of the ATT signal and the first deviation of a "straight line" behavior of the COD gauge output. This point can be easily seen in the differentiated ATT signal. A second differentiation of the COD gauge output would help to establish this point better. Such a second differentiation has not been attempted yet because of the relatively large noise level present in this signal. However, it is felt that the differentiated signals correlate in the unloading part of the load cycle: The differentiated ATT signal shows a zero slope at about 900N, a load in the vicinity of which the differentiated COD gauge output starts to increase (deviation from the dashed line). Using the approximately linear relationship between ATT output and the contact area at small ATT output levels (<3.5V) as shown in Fig. 12, it is possible to correlate the percentage of contact established from the ATT outputs with the COD gauge output shown in Fig. 19. The result is given in Fig. 21 for the data in Fig. 19 using the unloading part of the load cycle. The percentage of contact established is proportional to the COD gauge output until full contact has been established, as was pointed out in Section 1.1.

The results shown in Fig. 19, have characteristics which are quite similar to the ones observed during true crack closure, shown in Fig. 1. Naturally, the events are reversed. In the experiments, shown in Fig. 19, contact of the two faces is established at high load levels. On the other hand, true crack closure (Fig. 1) occurs at low load levels. Further experiments similar to the ones discussed in this section could be very fruitful for a full understanding of crack closure.

SC5032.22FR

IV. CONCLUSIONS

The present report summarizes the results of an effort devoted to compare the acoustic technique and the COD gauge technique used for crack closure measurements. Quantitative studies on the systems performances have been undertaken which show that the COD gauge, used in the present studies, performs as demonstrated in other studies (12). It is also shown that the two instruments measure two completely different quantities: The COD gauge yields information on the length change of the specimen whereas the acoustic signal is sensitive directly to the amount of contact area between the two surfaces interfering with the acoustic signal. This leads, basically to an advantage of the acoustic technique over the COD gauge technique: The COD gauge signal has to be processed, either by differentiation or by calculating "reduced displacements" (12) obtained from deviations from a straight line of best fit to the loading curve. Both the acoustic technique as well as the COD gauge technique work better on PTC than on CT specimens.

Compression tests have been performed by pressing a spherical cap (high strength aluminum) into a flat plate (well annealed 1100 Al) to determine the transmission of an acoustic signal as a function of contact area (determined optically). The transmitted signal was found to be approximately linear with the contact area (saturation of the electronic equipment is a major cause for deviations from linearity).

In another series of experiments two originally well annealed cylindrical Al specimens were pressed against each other and the transmitted acoustic signal as well as the displacement across the contacting faces determined using the COD gauge recorded as a function of load. These experiments have been designed to simulate crack closure. The results indicate that until 100% contact has been established the percentage of contact established is proportional to the COD gauge output.

SC5032.22FR

V. REFERENCES

- (1) W. Elber, in Damage Tolerance in Aircraft Structures, STP 486, American Society for Testing and Materials, Philadelphia (1971) p. 230.
- (2) R. A. Schmidt and P. C. Paris, in Progress in Flaw Growth and Fracture Toughness Testing, STP 536, American Society for Testing and Materials (1973), p. 79.
- (3) M. Katcher and M. Kaplan, in Fracture Toughness and Slow Stable Cracking, STP 559, American Society for Testing and Materials (1974), p. 264.
- (4) P. E. Irving, J. L. Robinson, and C. J. Beevers, International Journal of Fracture, 9, p. 105 (1973).
- (5) T. T. Shih and R. P. Wei, Engineering Fracture Mechanics, 6, p. 19 (1974).
- (6) T. C. Lindley and C. E. Richards, Materials Science and Engineering, 14, p. 281 (1974).
- (7) N. J. I. Adams, Engineering Fracture Mechanics, 4, p. 543 (1972).
- (8) W. N. Sharpe and A. F. Grandt, in Proceedings of the 20th International Instrumentation Symposium of the Instrument Society of America, Albuquerque, N.M. (May 1974).
- (9) O. Buck, C. L. Ho, H. L. Marcus, and R. B. Thompson, in Stress Analysis and Growth of Cracks, STP 513, American Society for Testing and Materials (1972) p. 280.
- (10) O. Buck, C. L. Ho, and H. L. Marcus, Engineering Fracture Mechanics, 5, p. 23 (1973).
- (11) J. D. Frandsen, R. V. Inman and O. Buck, Int. J. Fracture Mech., 11, 345 (1975).
- (12) W. Elber, Description of a Crack Opening-Displacement Gauge Measurement System, unpublished report.
- (13) O. Buck, J. D. Frandsen, C. L. Ho, and H. L. Marcus in Microstructure and Design of Alloys, Vol. I, The Institute of Metals and Iron and Steel Institute, 1973, p. 462.

FIGURE CAPTIONS

- Fig. 1 Comparison of closure curves on a CT specimen obtained from acoustic and compliance techniques.
- Fig. 2 Typical examples of the COD gauge and the differential COD gauge outputs as a function of load on a PTC specimen.
- Fig. 3 Typical examples of the ASWD and the differentiated ASWD outputs as a function of load on a PTC specimen.
- Fig. 4 Response of COD gauge as a function of load on a notched PTC specimen (notch depth a).
- Fig. 5 Response of the ASWD as a function of load on a notched PTC specimen (notch depth a).
- Fig. 6 Normalized stiffness and normalized ASWD output as a function of notch depth a .
- Fig. 7 Response of COD gauge as a function of load on a CT specimen for different saw cut depths a .
- Fig. 8 Response of the ATT as a function of load on a CT specimen for different saw cut depths a .
- Fig. 9 Disassembled compression jig. A and B are transducer holders (cylindrical specimen waxed to transducer holder at A, cavity for transducer shown at B). C is the well-annealed Al 1100 flat plate and D the Al 7075-T6 spherical cap. E is the teflon guide piece, and F the COD gauge.
- Fig. 10 Assembled compression jig.
- Fig. 11 Typical example of the ATT output as a function of load during a compression test (spherical cap against flat plate). The insert shows a picture of the impression left in the flat plate.
- Fig. 12 Saturation signal level (ATT output at maximum load) and average stress level as a function of contact area.
- Fig. 13 Contact area as a function of average applied stress level. P_{max} indicates the maximum applied load achieved during test.
- Fig. 14 COD gauge and ATT output as a function of load. Full contact of cylinders not established yet.
- Fig. 15 COD gauge and ATT output as a function of load. Full contact of cylinders almost established.
- Fig. 16 COD gauge and ATT output as a function of load. Full contact of cylinders just established.
- Fig. 17 COD gauge and ATT output as a function of load. Full contact of cylinders far exceeded.

- Fig. 18 COD gauge and ATT output as a function of load as the maximum load exceeds the yield stress of the material.
- Fig. 19 COD gauge and ATT output as a function of load. Material was work hardened at higher stress level before test. Compare with Fig. 17.
- Fig. 20 Differentiated signals of Fig. 19. Note the feathered arrow indicating the most likely position of full closure.
- Fig. 21 Percentage of contact established (using the ATT output) as a function of COD gauge output.

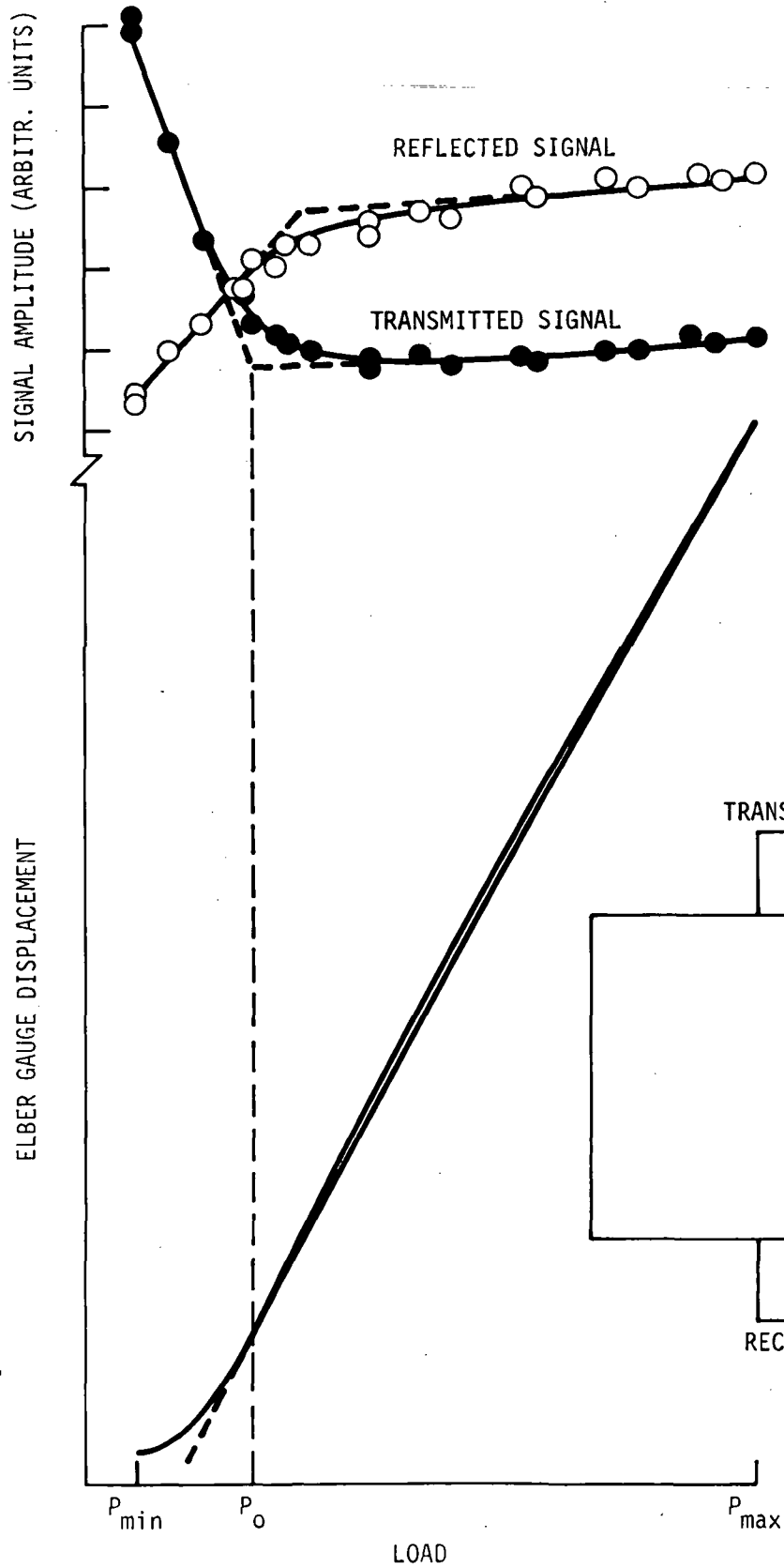


Figure 1

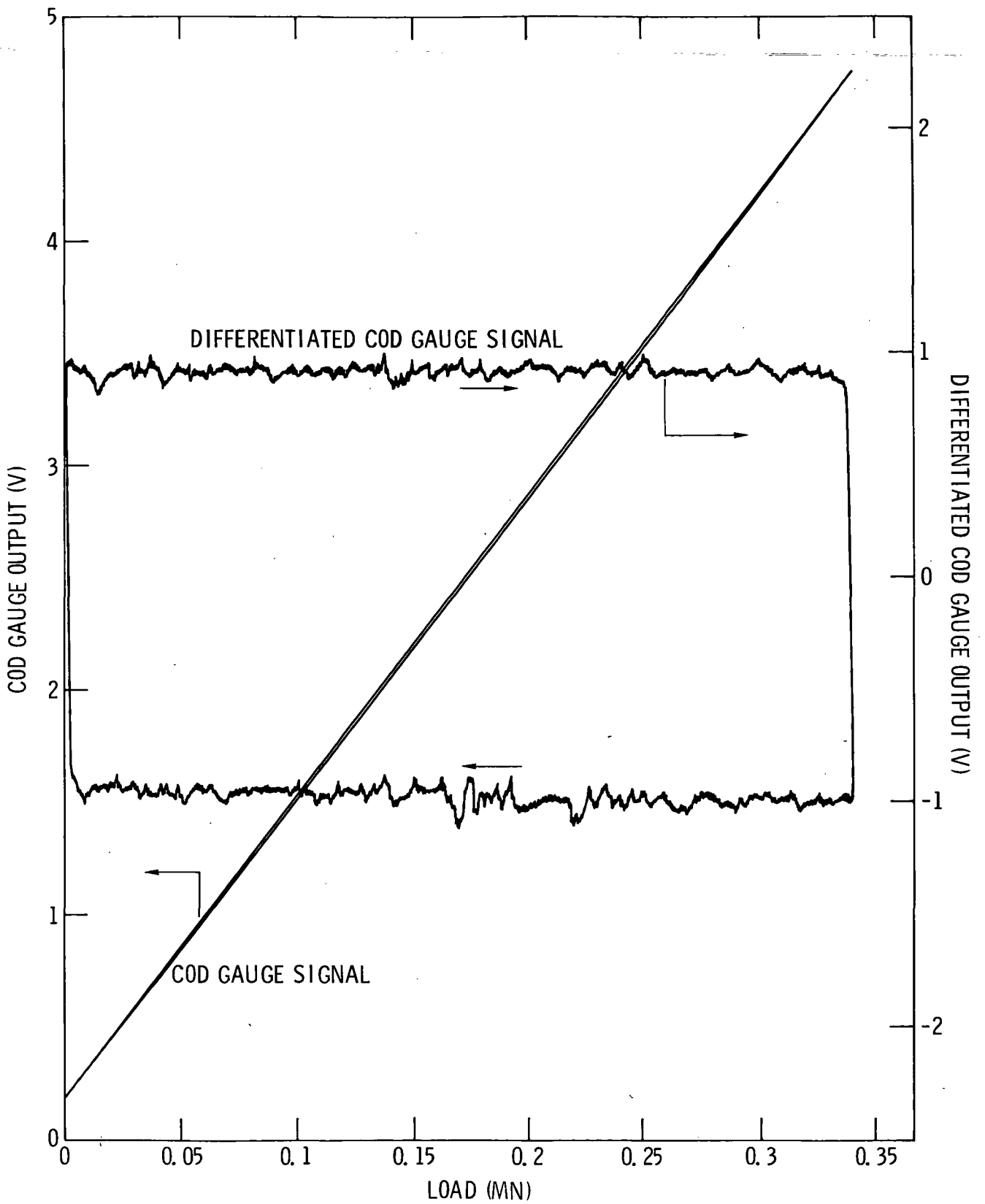


Figure 2

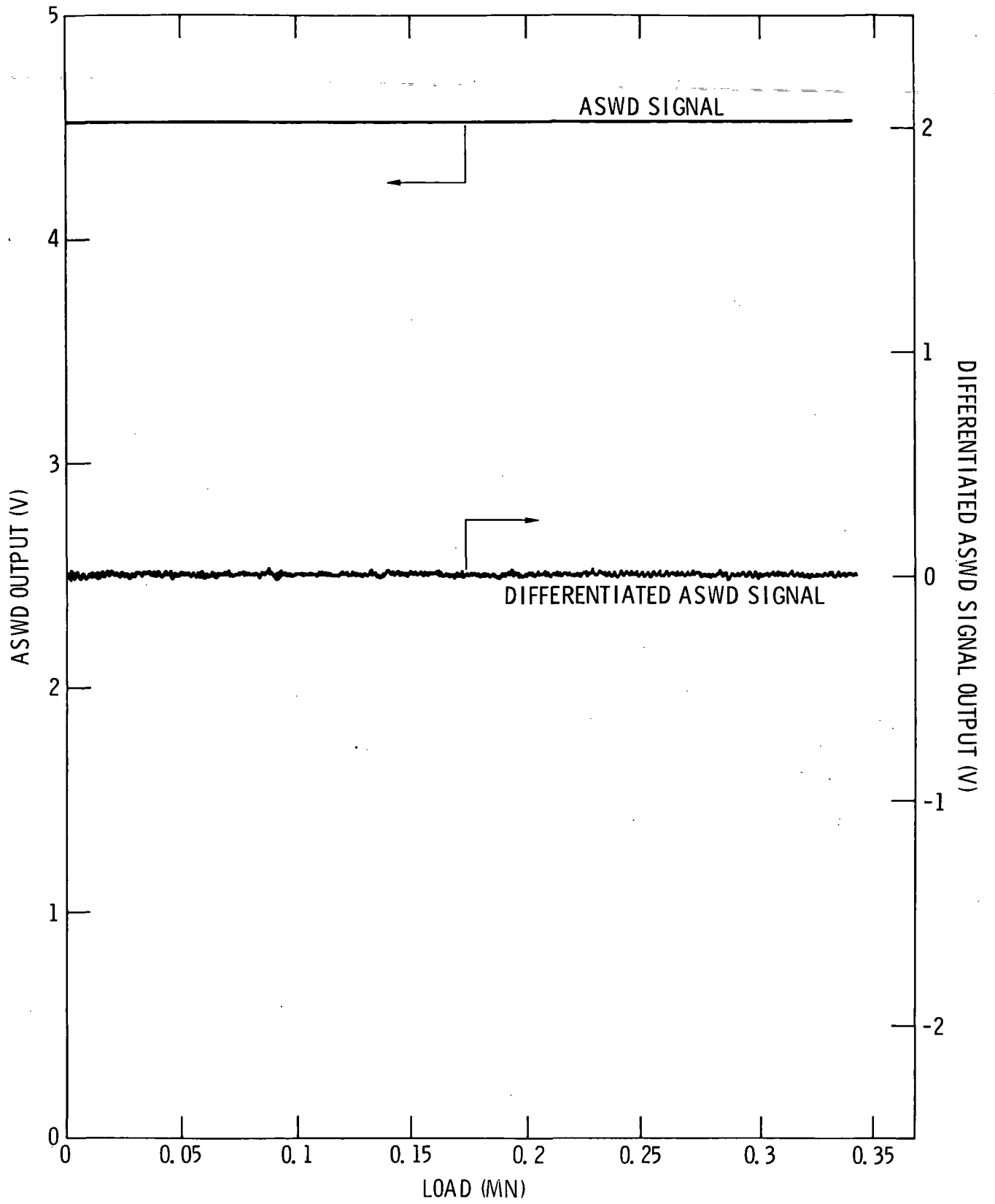


Figure 3

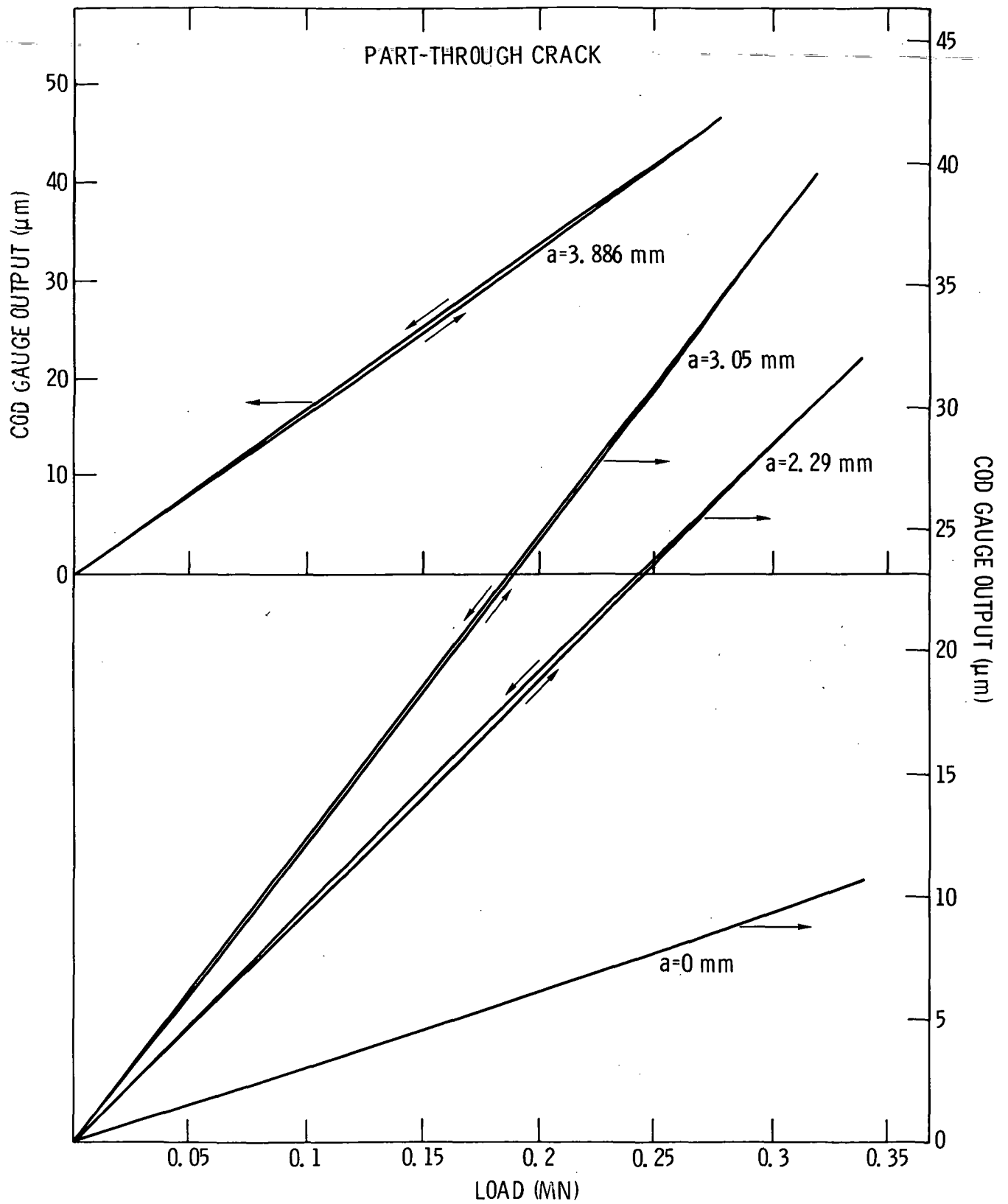


Figure 4

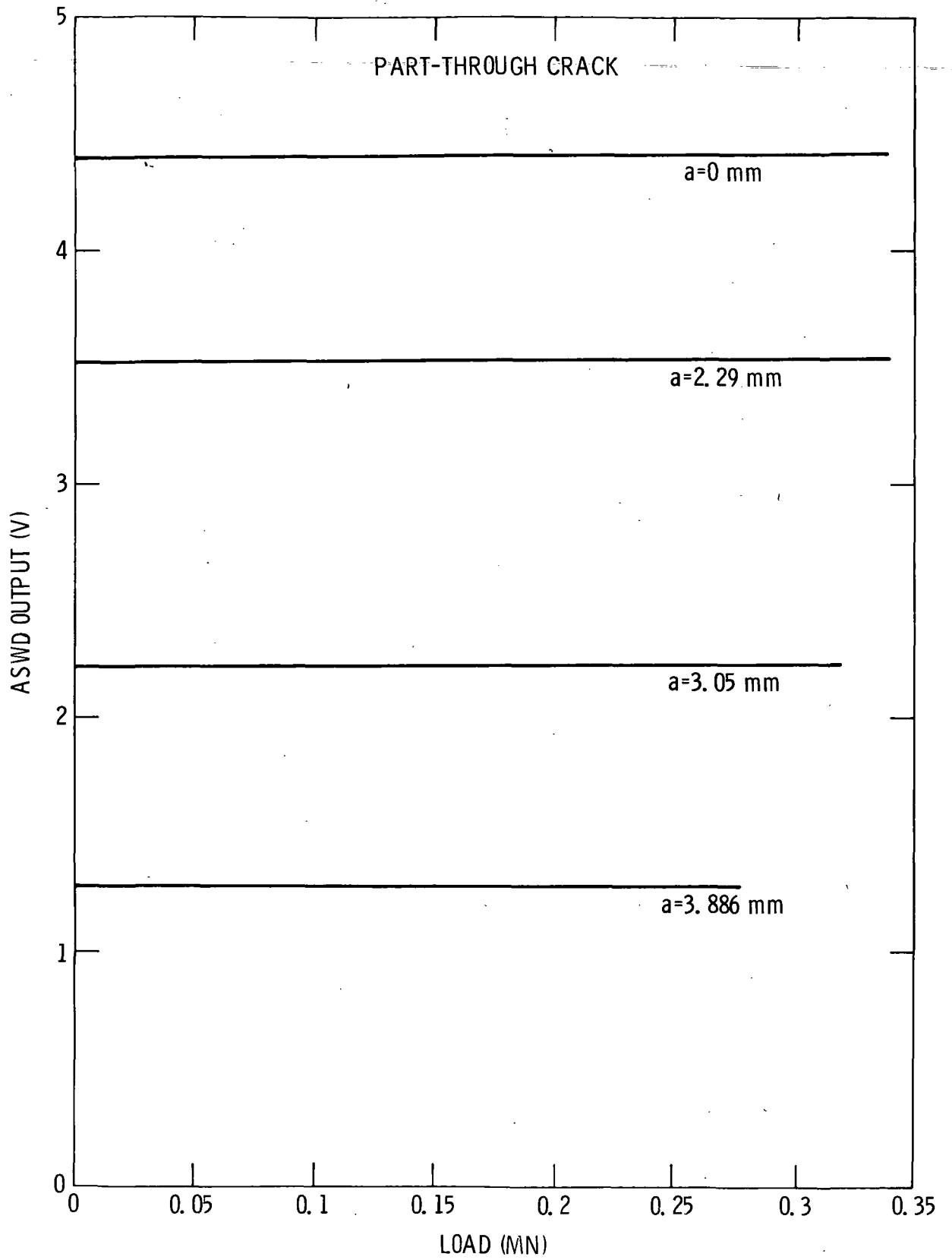


Figure 5

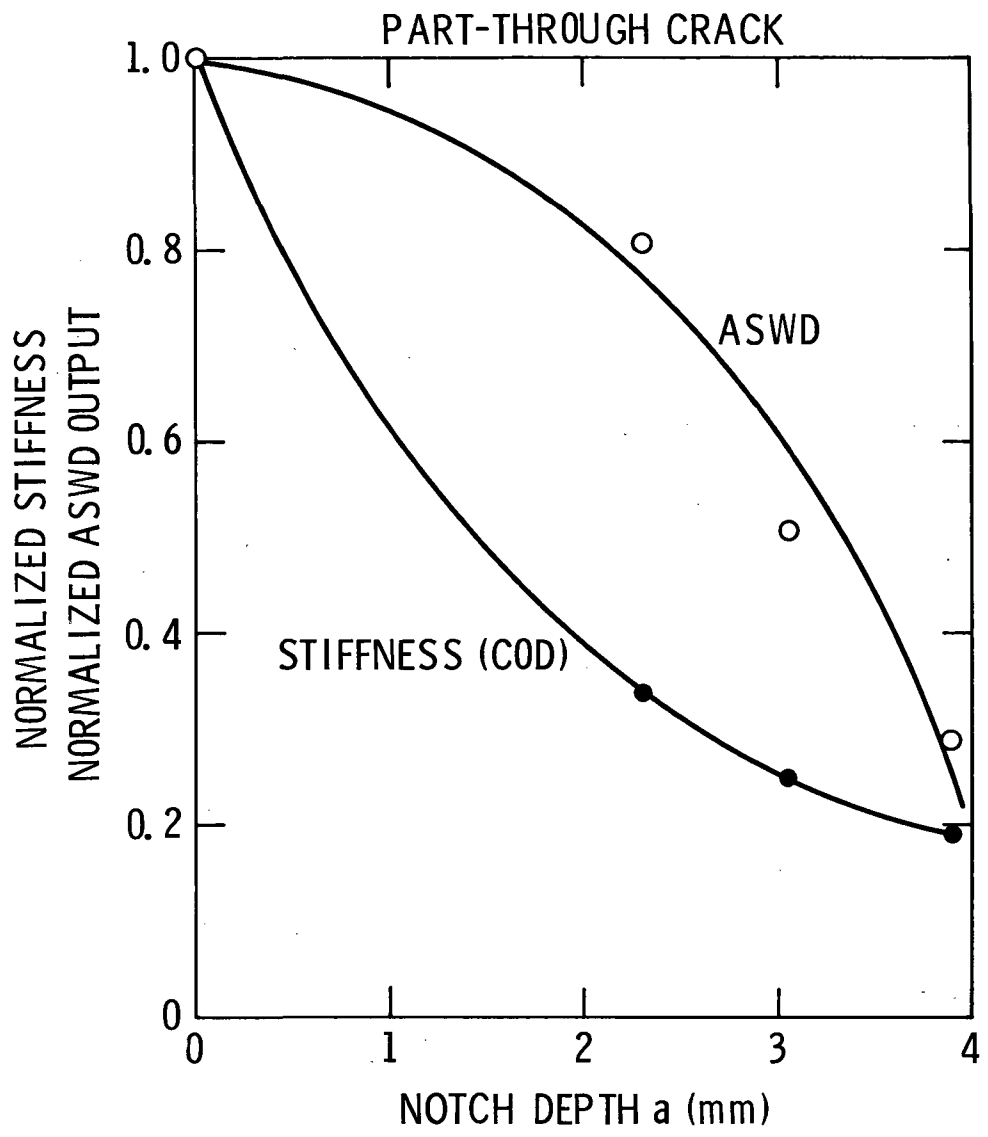


Figure 6

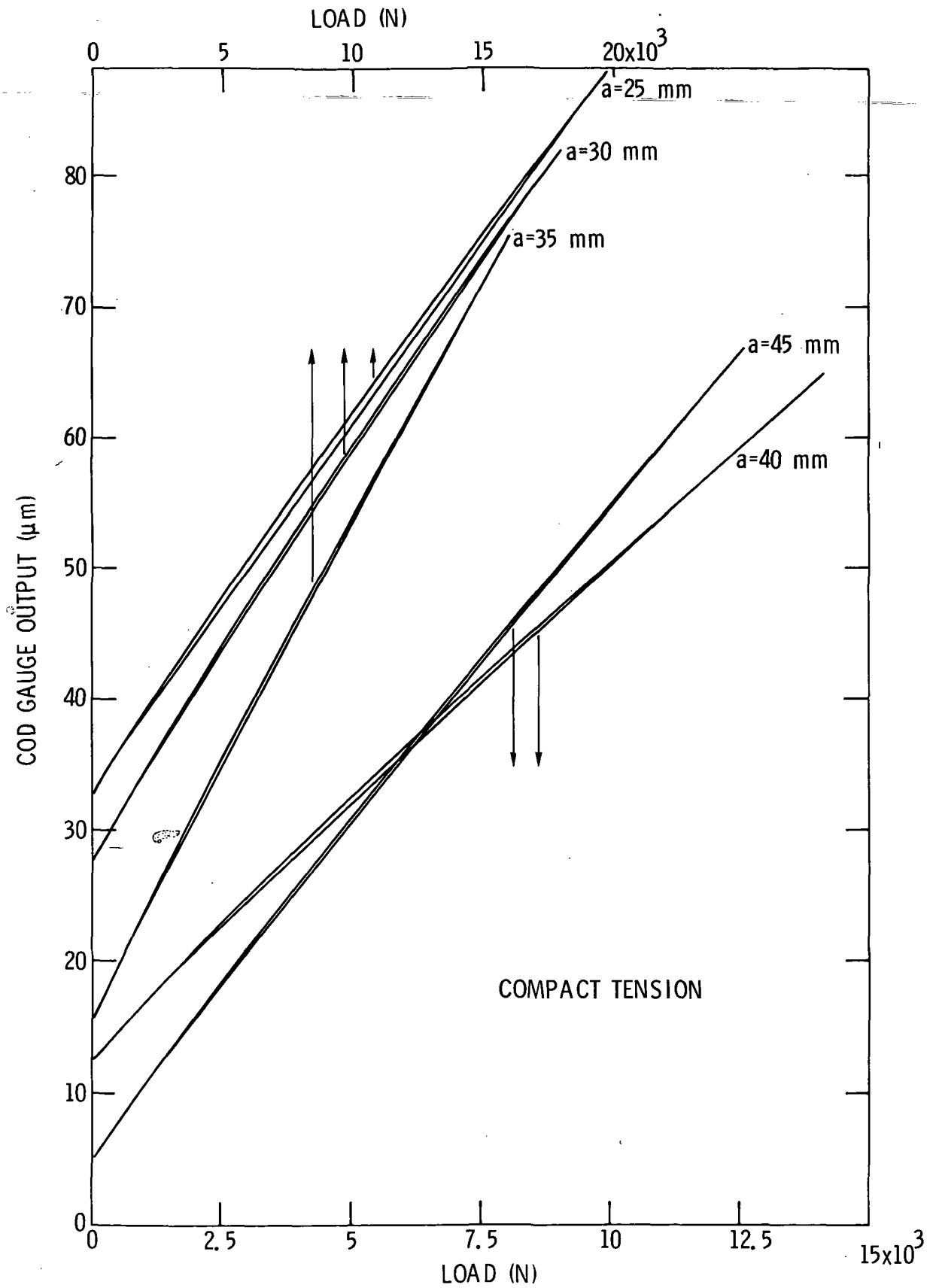


Figure 7.

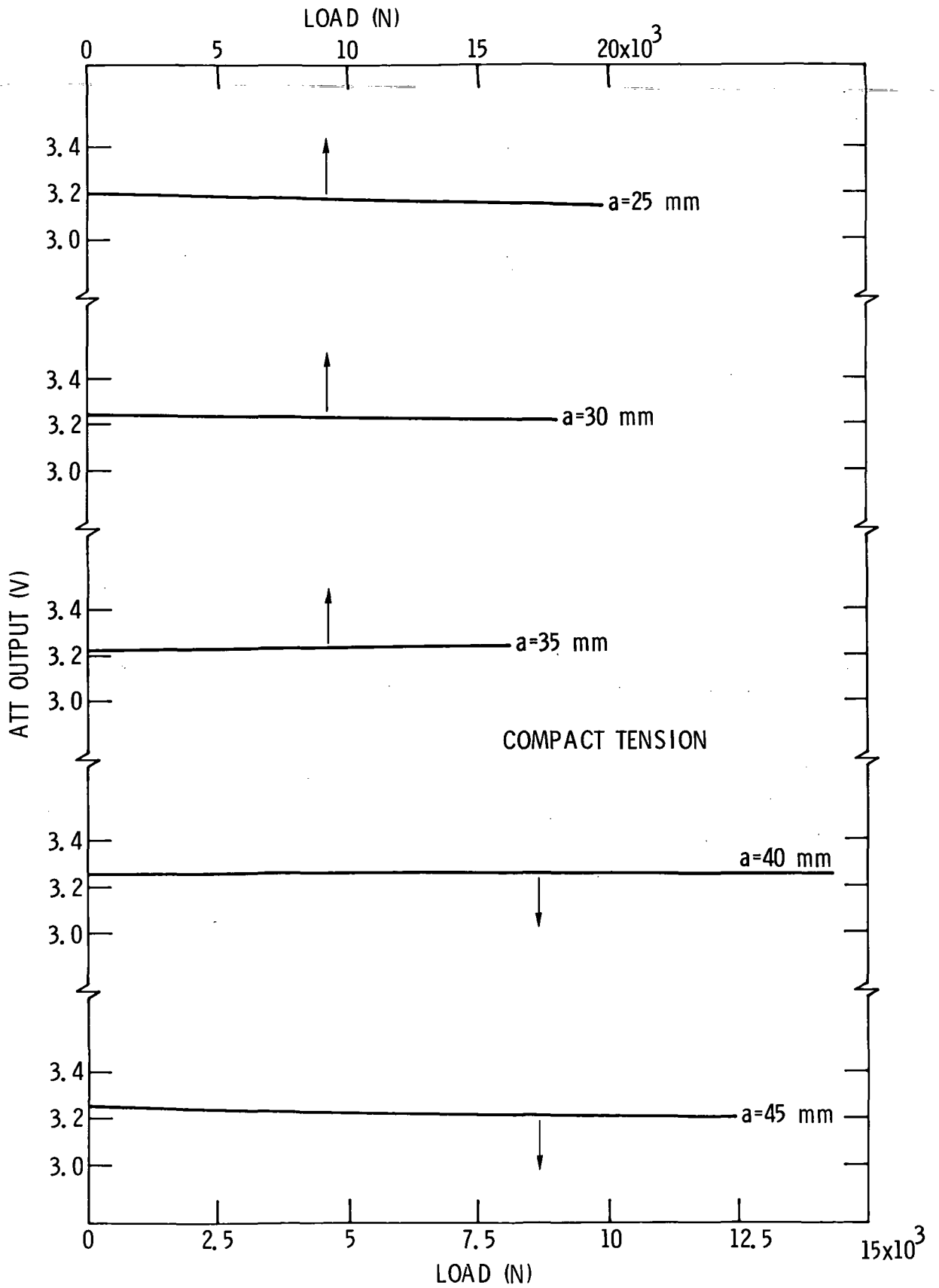


Figure 8

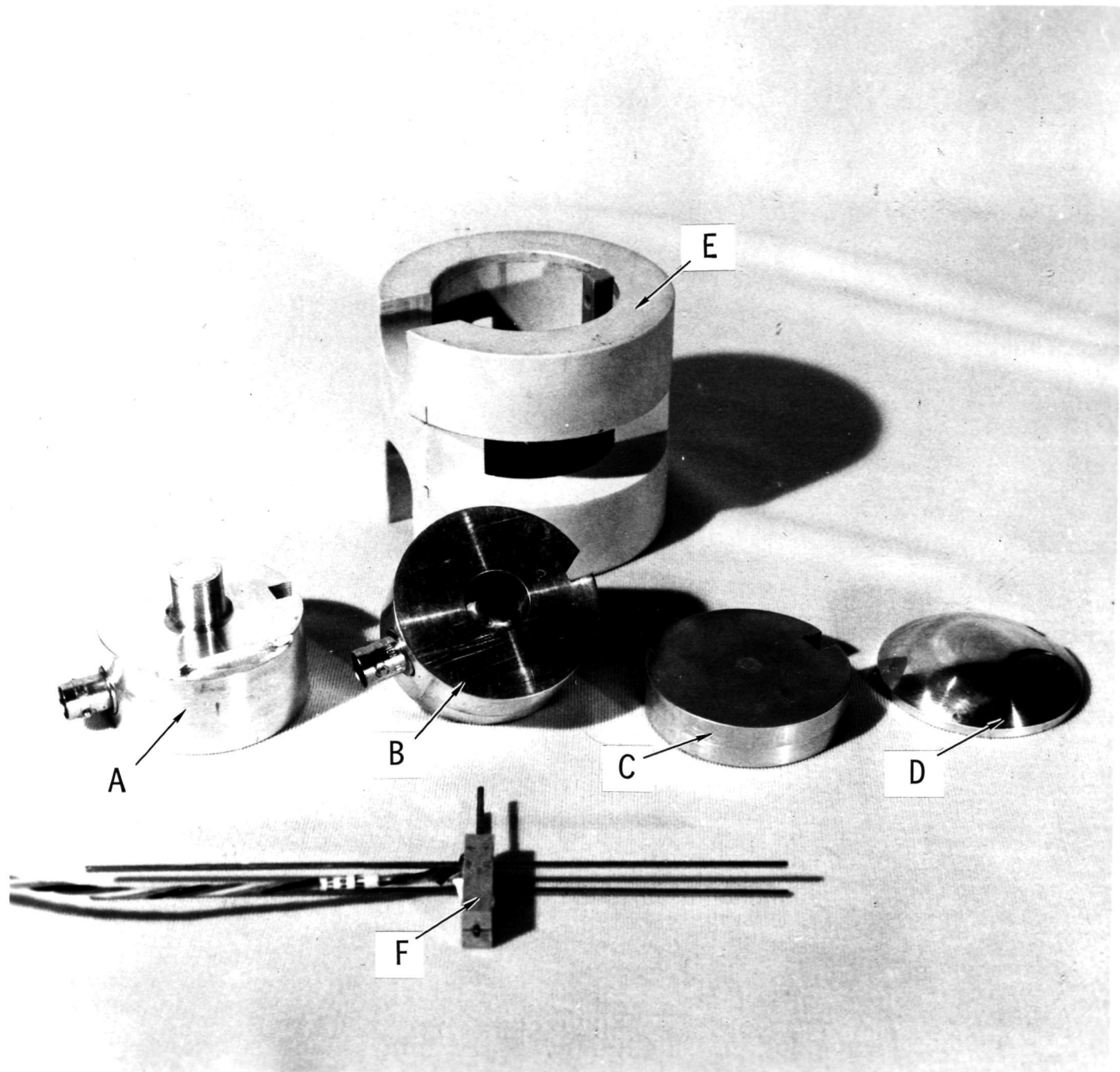


Figure 9

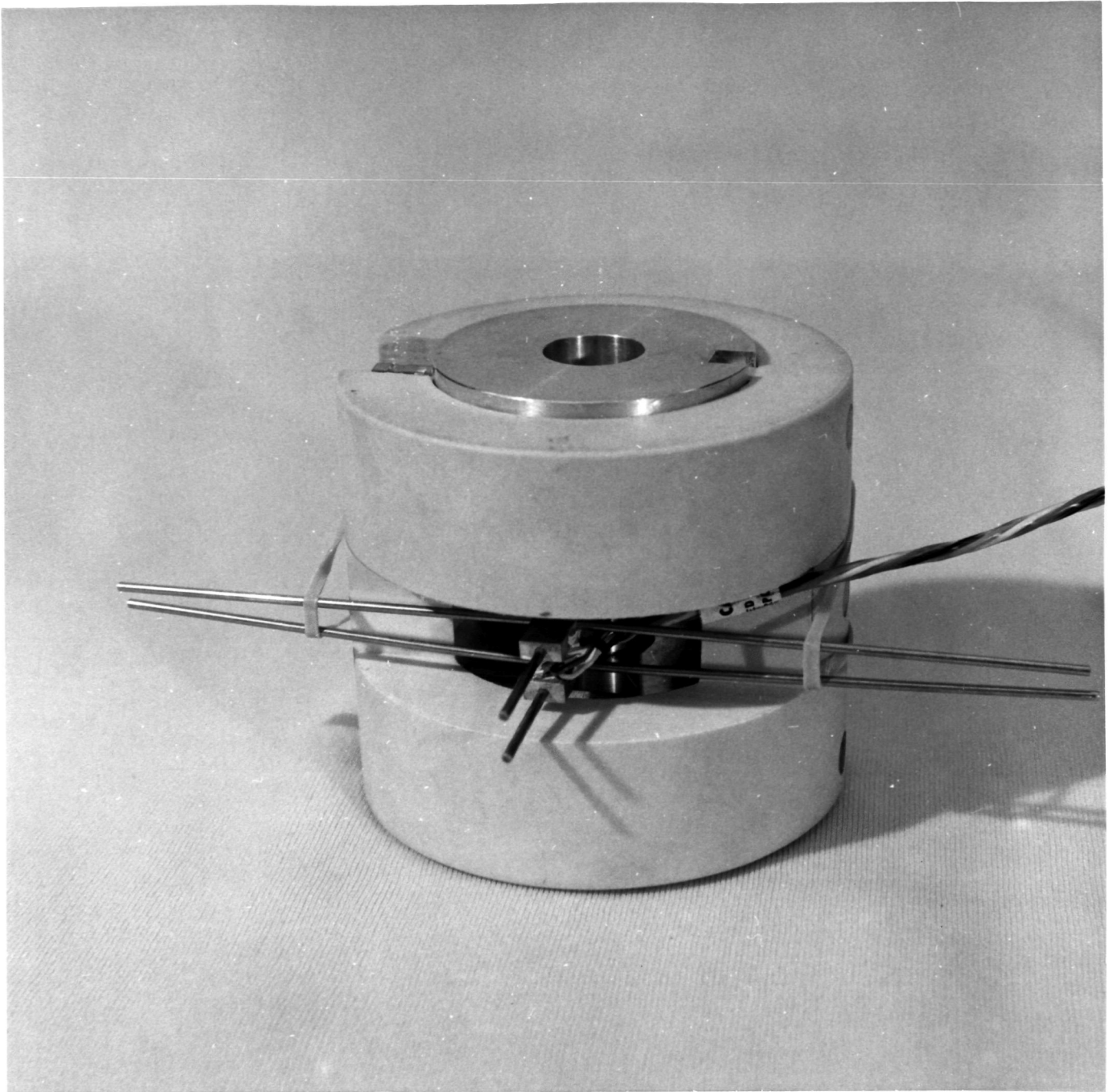


Figure 10

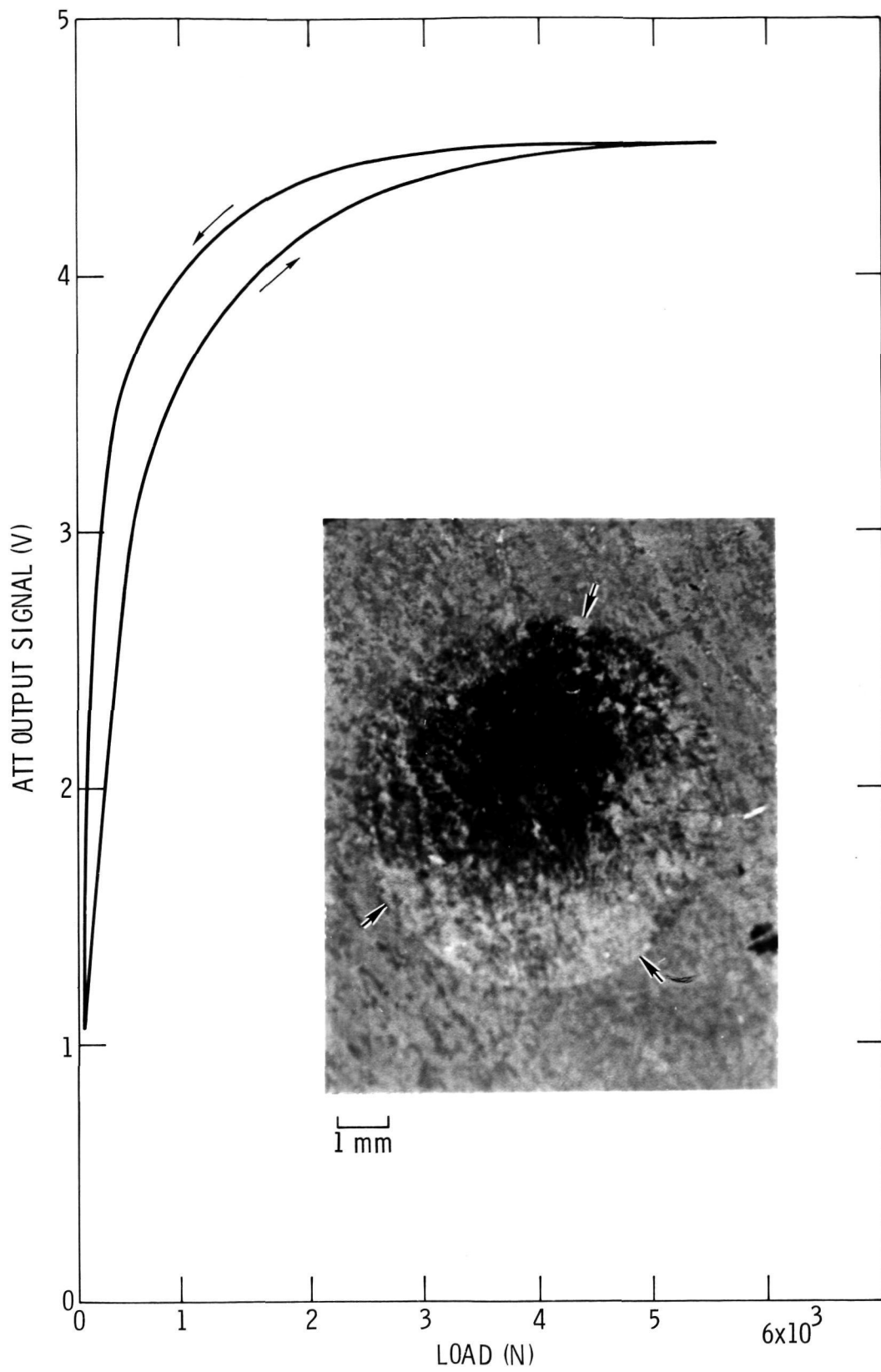


Figure 11

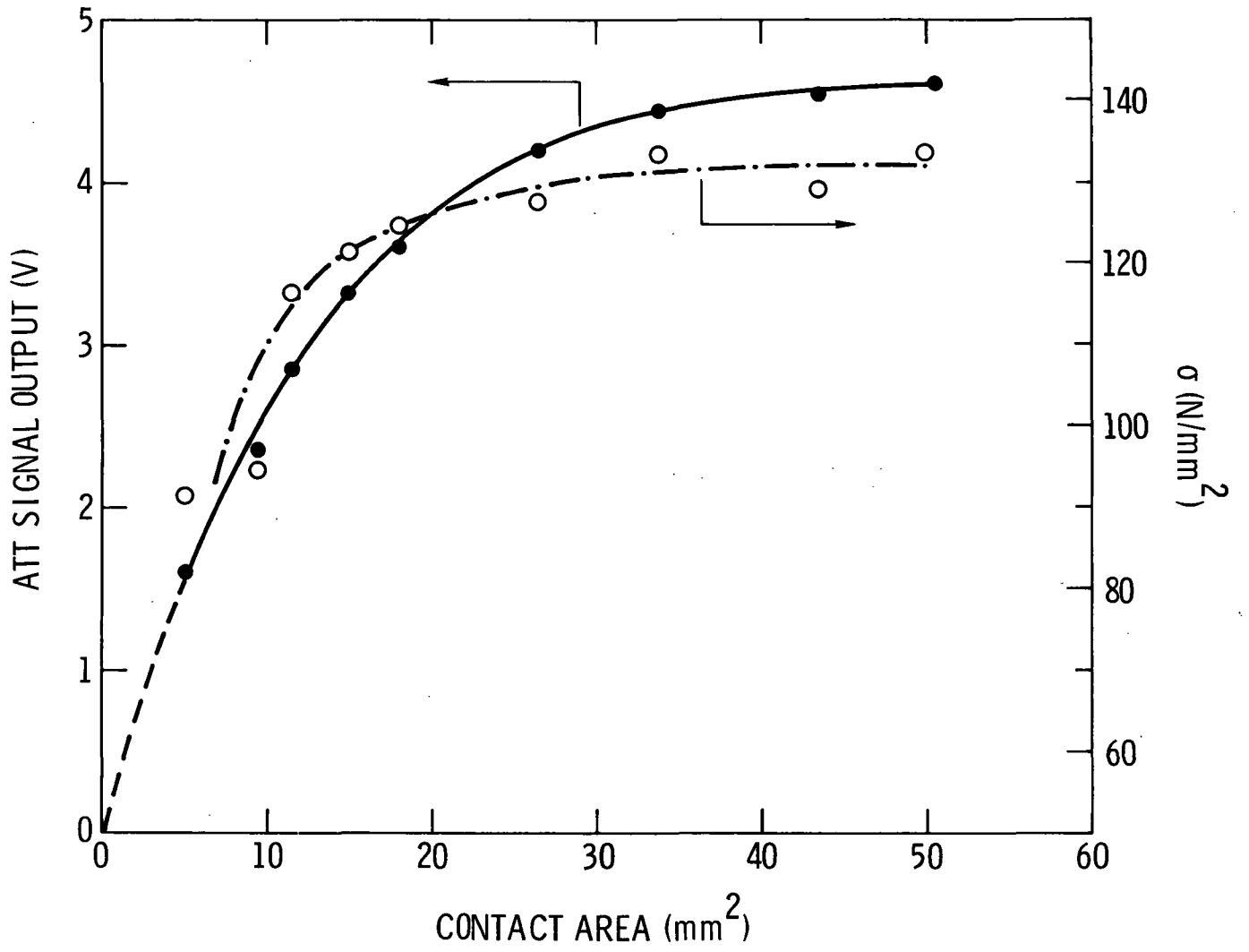


Figure 12

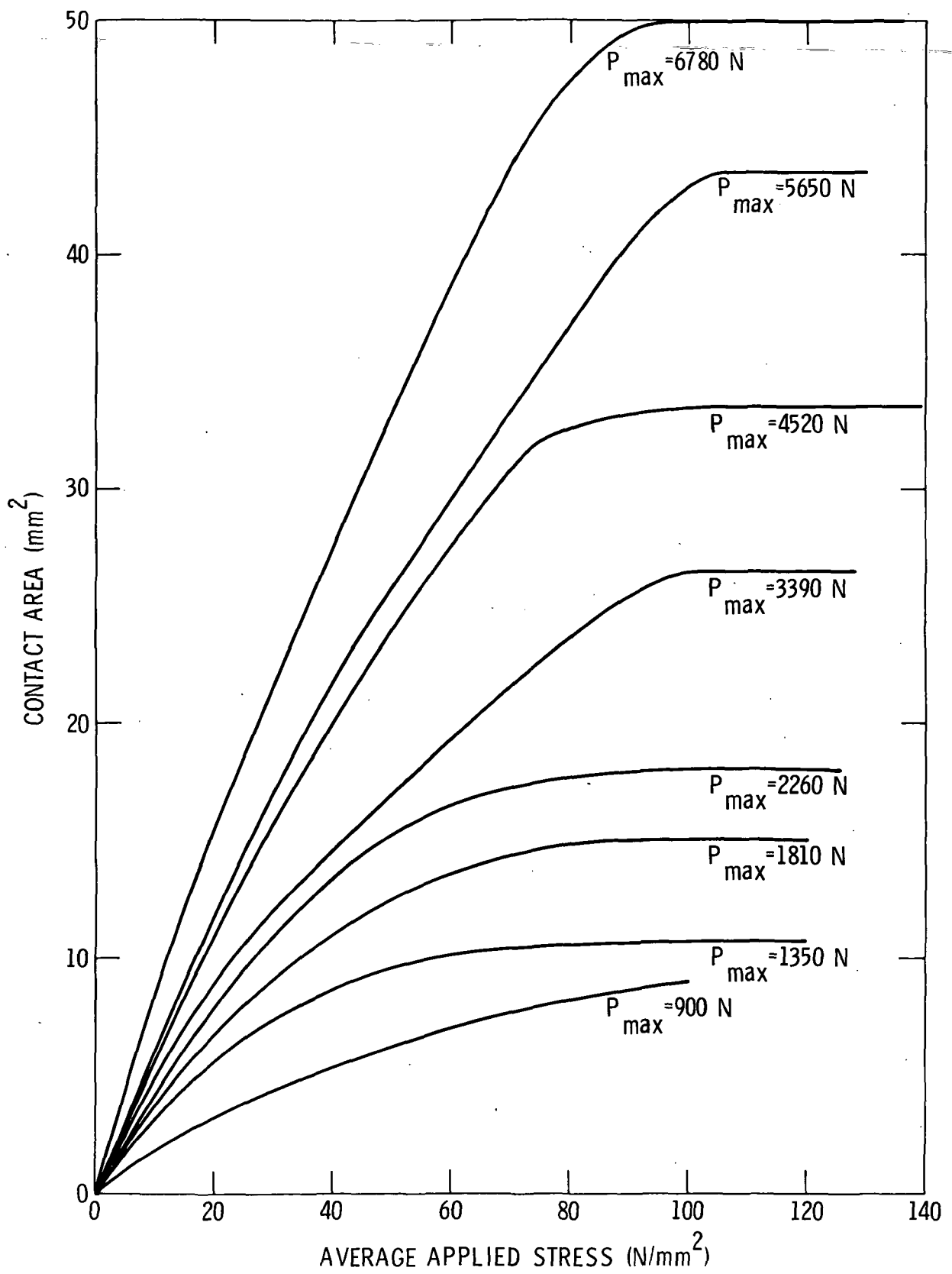


Figure 13

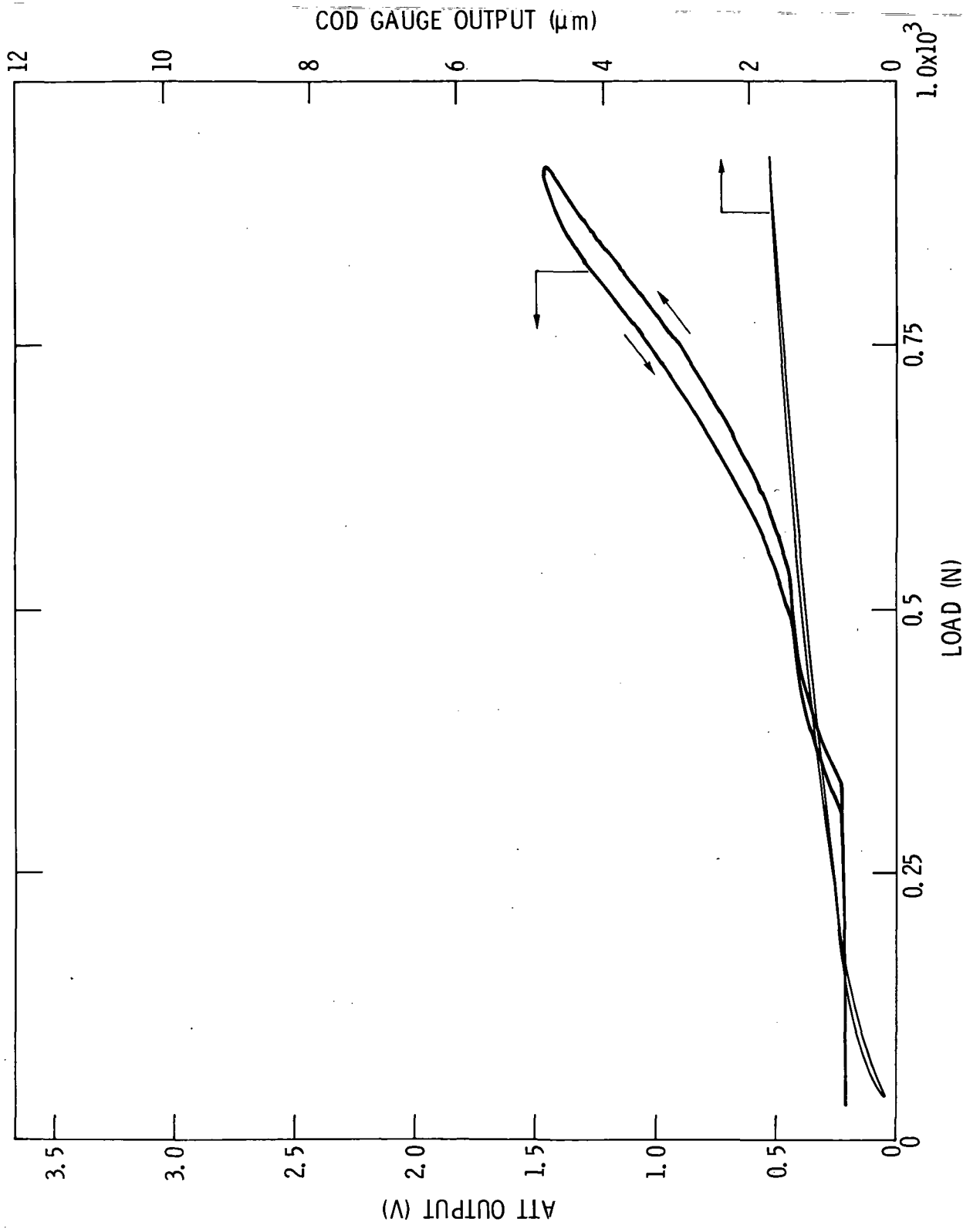


Figure 14

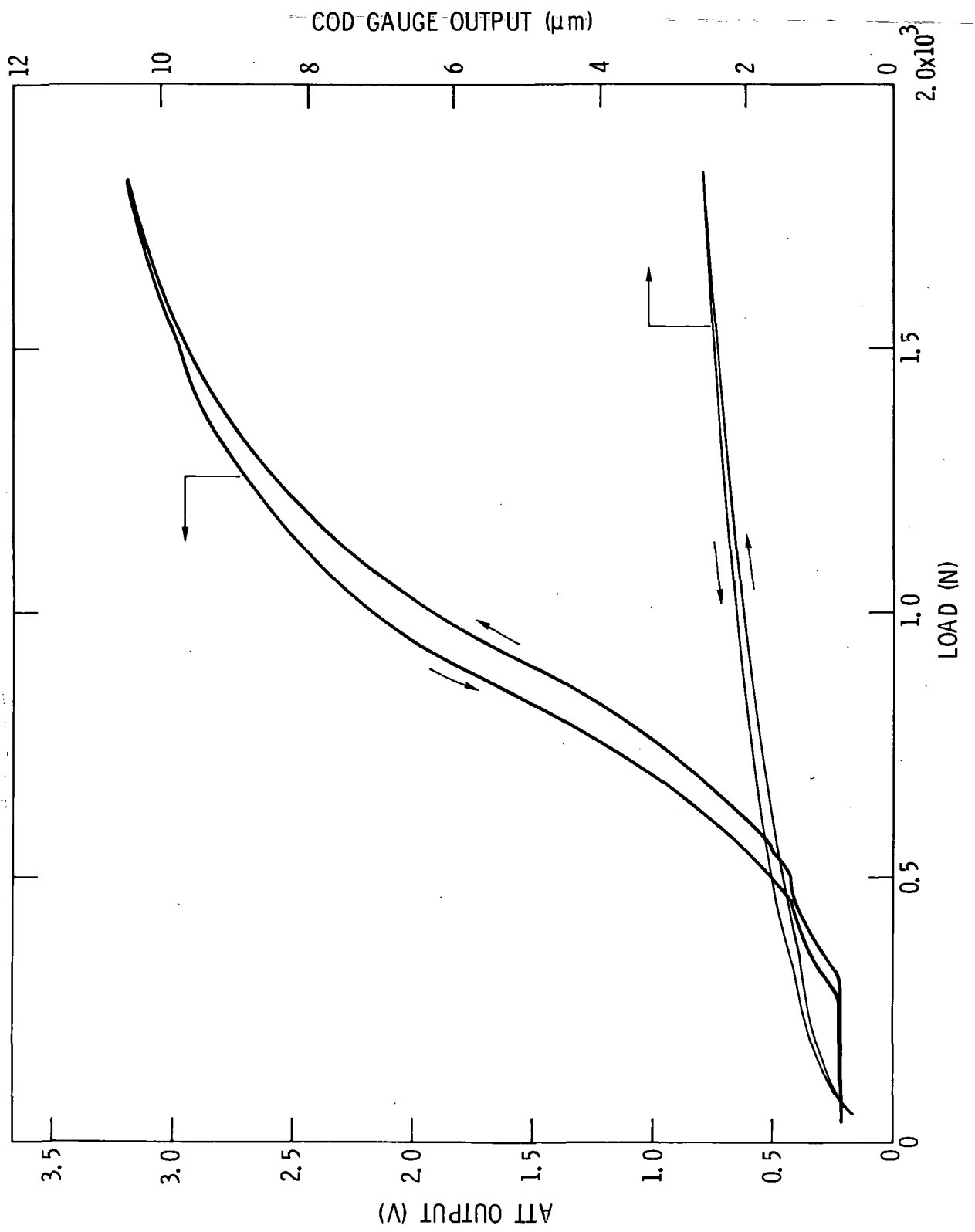


Figure 15

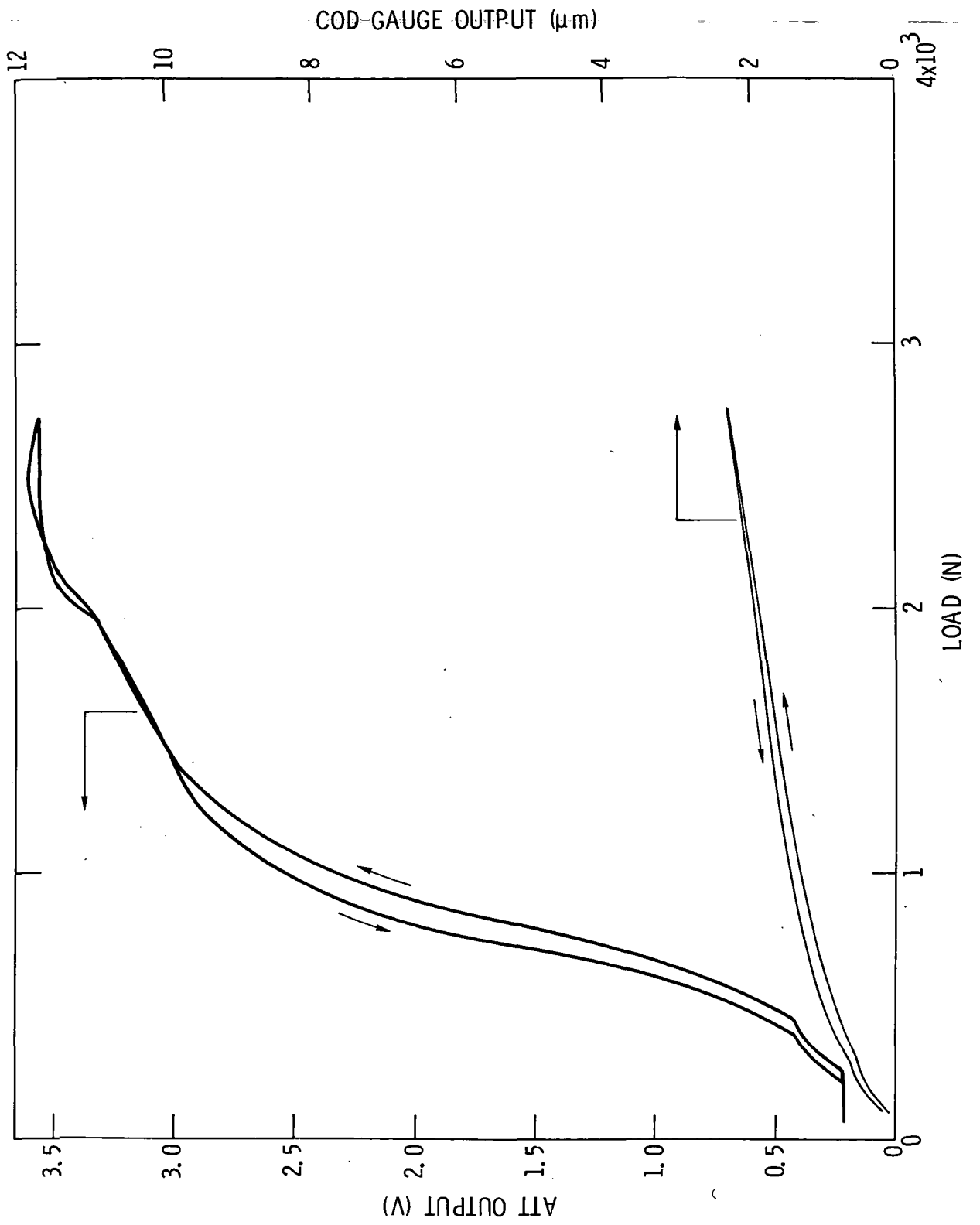


Figure 16

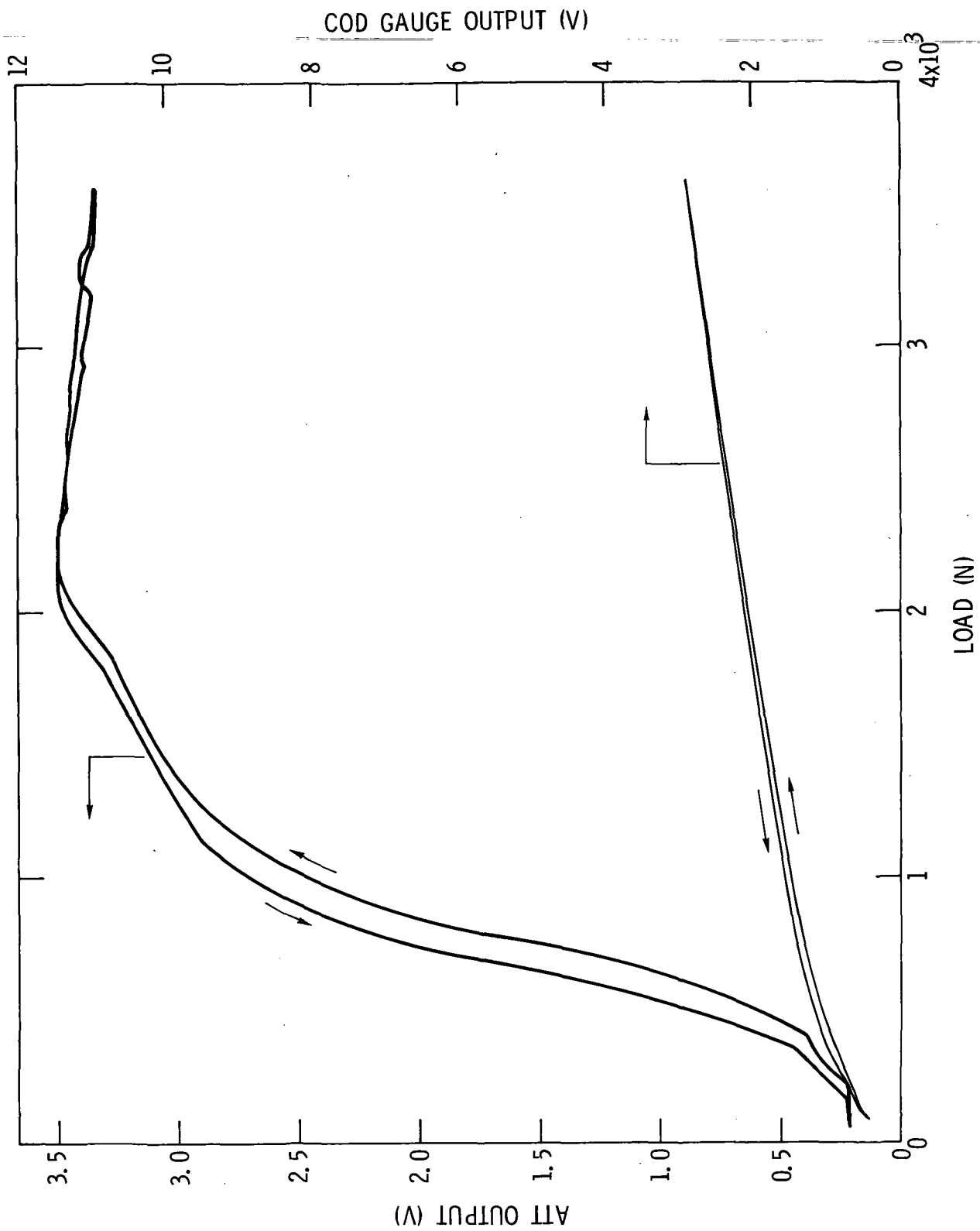


Figure 17

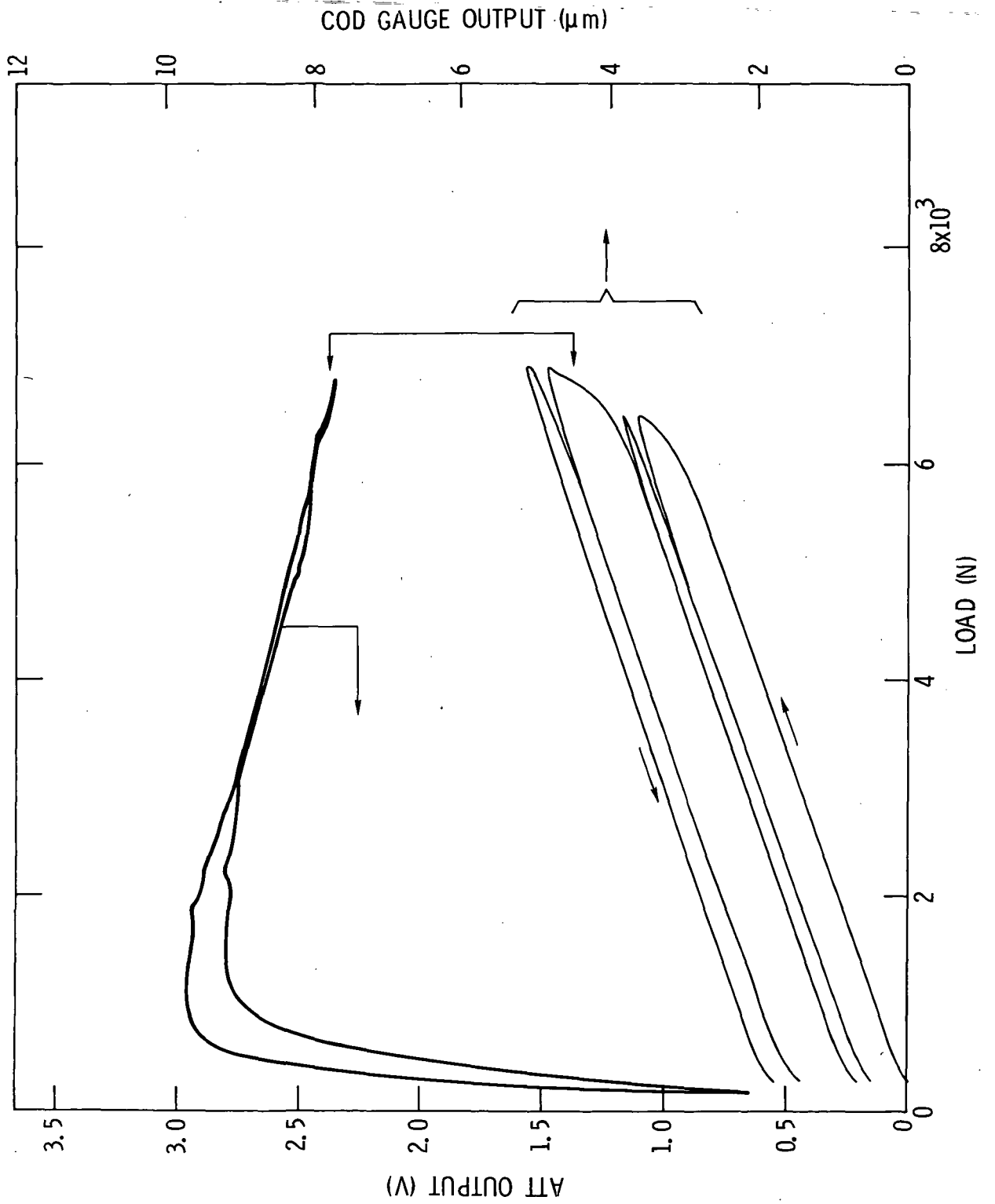


Figure 18

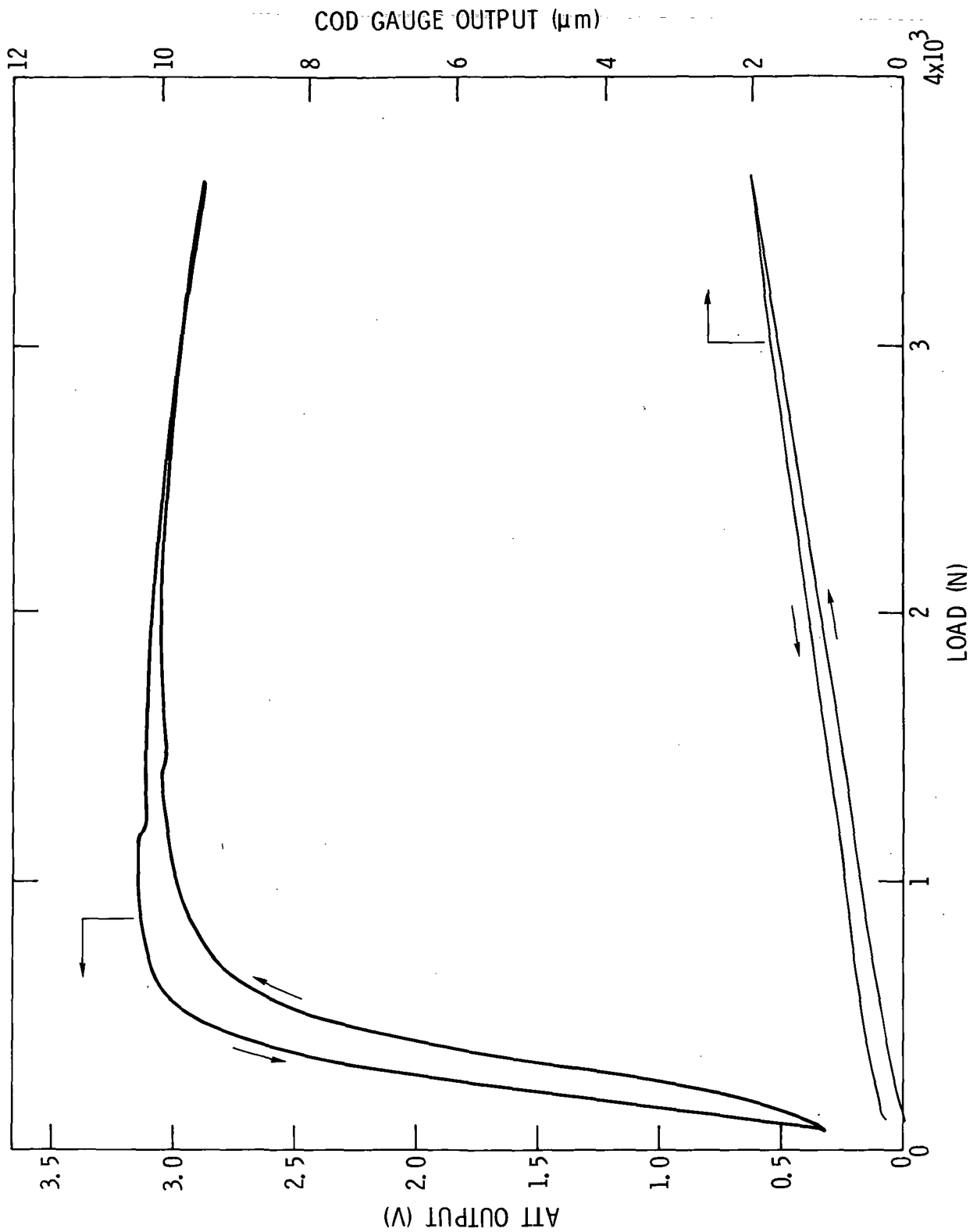


Figure 19

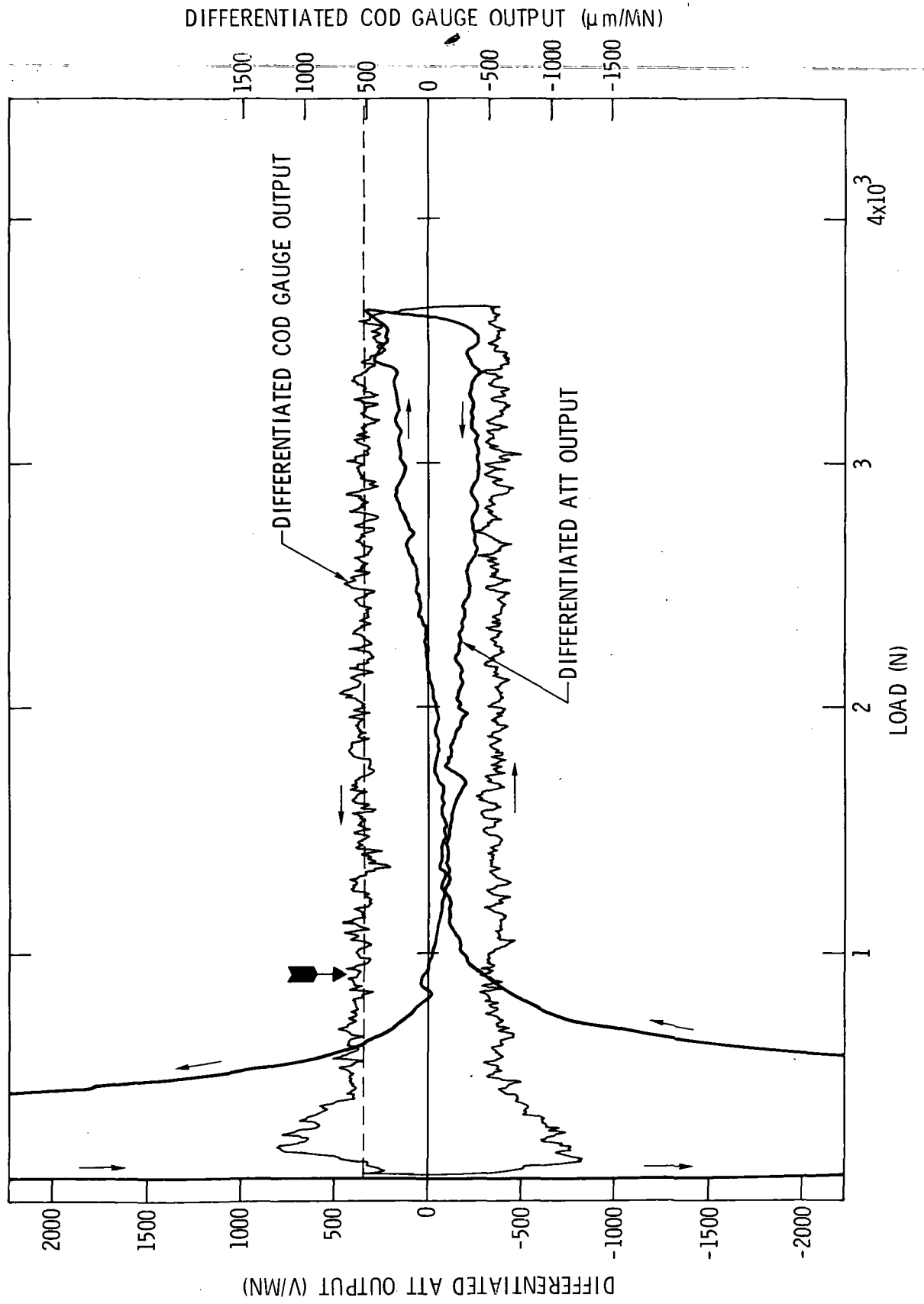


Figure 20

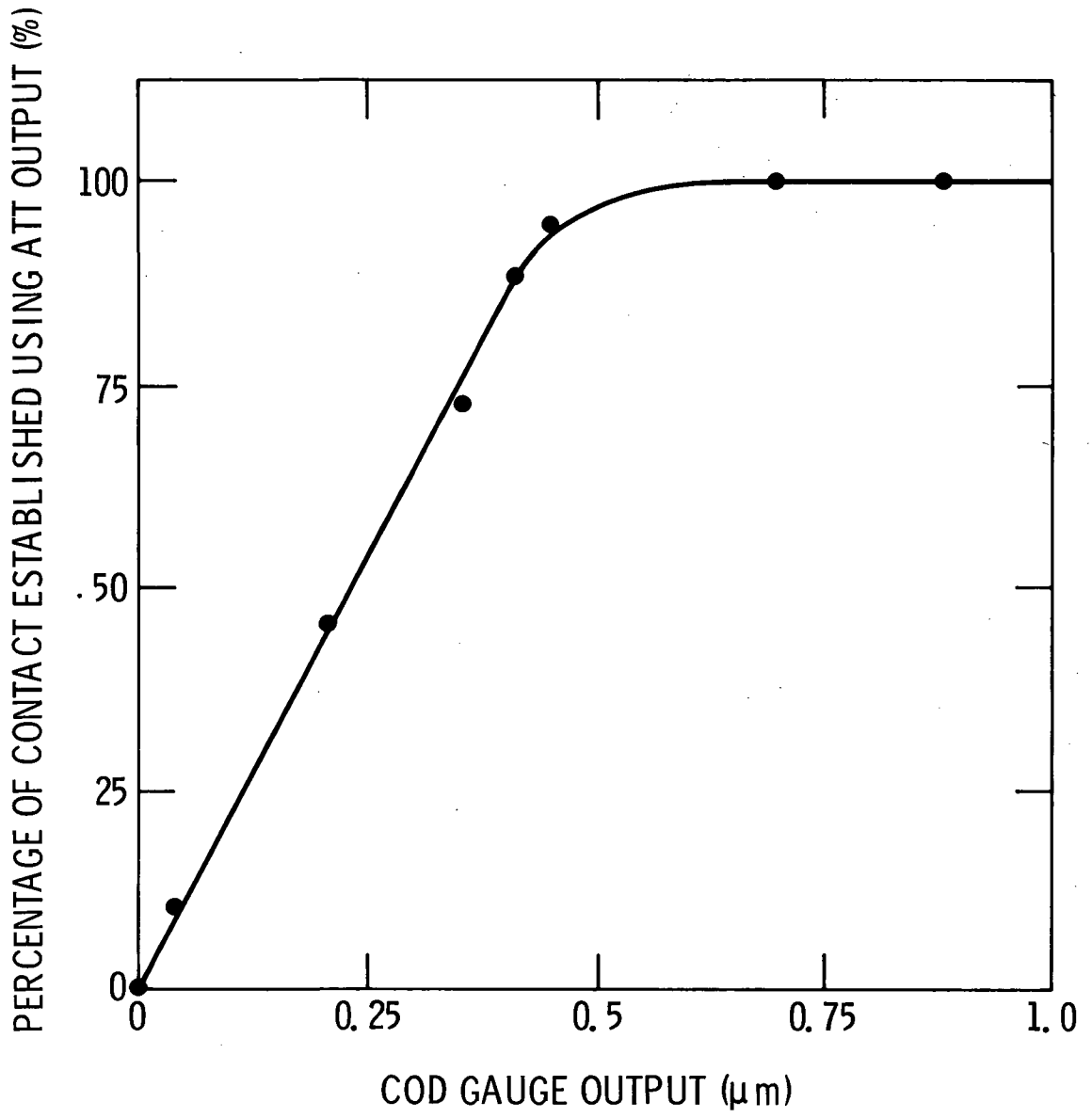


Figure 21